

This is a repository copy of *Water-Soluble Organic Composition of the Arctic Sea Surface Microlayer and Association with Ice Nucleation Ability*.

White Rose Research Online URL for this paper:

<https://eprints.whiterose.ac.uk/id/eprint/127892/>

Version: Accepted Version

Article:

Chance, Rosemary Jane orcid.org/0000-0002-5906-176X, Hamilton, Jacqueline Fiona orcid.org/0000-0003-0975-4311, Carpenter, Lucy Jane orcid.org/0000-0002-6257-3950 et al. (3 more authors) (2018) Water-Soluble Organic Composition of the Arctic Sea Surface Microlayer and Association with Ice Nucleation Ability. *Critical Reviews in Environmental Science and Technology*. pp. 1817-1826. ISSN: 1547-6537

<https://doi.org/10.1021/acs.est.7b04072>

Reuse

Items deposited in White Rose Research Online are protected by copyright, with all rights reserved unless indicated otherwise. They may be downloaded and/or printed for private study, or other acts as permitted by national copyright laws. The publisher or other rights holders may allow further reproduction and re-use of the full text version. This is indicated by the licence information on the White Rose Research Online record for the item.

Takedown

If you consider content in White Rose Research Online to be in breach of UK law, please notify us by emailing eprints@whiterose.ac.uk including the URL of the record and the reason for the withdrawal request.

1 Water-soluble organic composition of the
2 Arctic sea surface microlayer and association
3 with ice nucleation ability

4

5 *Rosie J. Chance*^{*1}, *Jacqueline F. Hamilton*¹, *Lucy J. Carpenter*¹, *Sina C.*

6 *Hackenberg*¹, *Stephen J. Andrews*¹, *Theodore W. Wilson*^{2†}

7

8 1. Wolfson Atmospheric Chemistry Laboratories, Department of Chemistry,

9 University of York, Heslington, York, YO10 5DD, UK.

10 2. School of Earth and Environment, University of Leeds, Woodhouse Lane, Leeds,

11 LS2 9TJ, UK.

12

13 †Now at Owlstone Medical Ltd., 162 Cambridge Science Park, Milton Road

14 Cambridge, CB4 0GH, UK.

15

16

17 * Corresponding author: rosie.chance@york.ac.uk

18

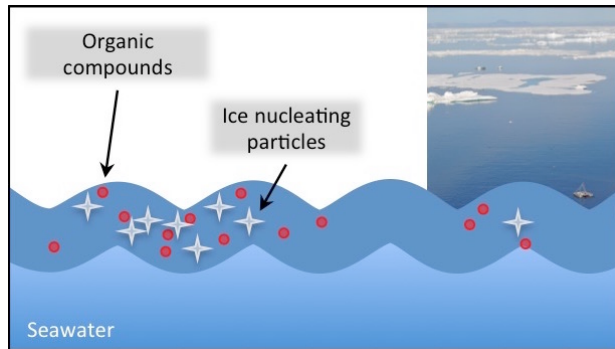
19 **Abstract**

20 Organic matter in the sea surface microlayer (SML) may be transferred to the
21 atmosphere as sea spray and hence influence the composition and properties of
22 marine aerosol. Recent work has demonstrated that the SML contains material
23 capable of heterogeneously nucleating ice, but the nature of this material remains
24 largely unknown. Water-soluble organic matter was extracted from SML and
25 underlying seawater from the Arctic and analyzed using a combination of mass
26 spectrometric approaches. High performance liquid chromatography-ion trap mass
27 spectrometry (LC-IT-MS), and Fourier transform ion cyclotron resonance MS (FT-
28 ICR-MS), showed seawater extracts to be compositionally similar across all stations,
29 while microlayer extracts had a different and more variable composition. LC-IT-MS
30 demonstrated the enrichment of particular ions in the microlayer. Ice nucleation
31 ability (defined as the median droplet freezing temperature) appeared to be related to
32 the relative abundances of some ions, although the extracts themselves did not retain
33 this property. Molecular formulae were assigned using LC - quadrupole time-of-flight
34 MS (LC-TOF-MS²) and FT-ICR-MS. The ice nucleation tracer ions were associated
35 with elevated biogenic trace gases, and were also observed in atmospheric aerosol
36 collected during the summer, but not early spring suggesting a biogenic source of ice
37 nuclei in the Arctic microlayer.

38

39

40 **TOC/Abstract art**



41

42 **Introduction**

43 The sea surface microlayer (SML) is a thin layer of water at the sea-air interface in
44 which chemical, physical and biological properties differ from those of the underlying
45 seawater¹. The SML has an operationally defined thickness of ~1 to ~1000 μm ¹, and
46 surfactant enrichments have been found to persist up to wind speeds of up to at least ~
47 13 m s^{-1} ^{2, 3}. It has been recognized as a distinct compartment for photochemical
48 reactions^{4, 5} and biogeochemical transformations¹.

49
50 As the SML lies at the interface between the ocean and the atmosphere, it is expected
51 to influence the transfer of gases and particles between these compartments⁶⁻¹⁰.
52 Material from the SML may become entrained in sea spray aerosol (SSA) generated
53 by bubble bursting processes¹¹, but the extent of the SML's direct contribution to SSA
54 remains unknown¹². In the central Arctic, atmospheric particles have been found to
55 have similar properties to particles (~100 nm diameter) in the SML beneath,
56 suggesting that the SML may be a significant source of these aerosol particles¹³.
57 Similarly, co-variation of anionic surfactants in aerosol and the SML in the
58 Mediterranean suggests the SML is a source of aerosol organic matter¹⁴.
59 Photochemical and heterogeneous reactions in the microlayer may also supply
60 volatile organic compounds (VOCs) to the atmosphere, and so contribute to
61 secondary organic aerosol formation^{4, 15, 16}.

62
63 The influence of the SML on air-sea exchange and marine aerosol properties is
64 assumed to be a function of its chemical composition, but as yet, the composition of
65 the microlayer has not been fully characterized. Relative to the underlying bulk
66 seawater, the SML has been found to be enriched in a wide range of organic and

67 inorganic compounds (¹² and references therein; ^{6, 17-27}). Rising bubbles collect surface-
68 active organic material from the water column and transfer it to the microlayer^{1, 2},
69 where further enrichment and/or modification (e.g. by photochemical oxidation⁵, or
70 microbial degradation^{1, 28}) of some compound classes may occur. Non-targeted high-
71 resolution mass spectrometry has shown a shift towards lower molecular weight
72 compounds in the SML relative to the underlying seawater, thought to be the result of
73 increased degradation²².

74

75 The microlayer is also enriched in biogenic material that can heterogeneously
76 nucleate ice²⁹. The presence of ice nucleating particles (INPs) in bulk seawater and
77 marine air masses has long been known³⁰⁻³⁵, and recent studies indicate that the oceans
78 are probably an important source of aerosolized atmospheric INPs, particularly in
79 remote regions away from terrestrial sources^{29, 36-38}. Depending on the exact nucleation
80 pathway, heterogeneous ice nucleation by INPs can raise the temperature and/or
81 lower the relative humidity at which ice crystals form in clouds, with consequent
82 impacts on cloud lifetime, precipitation and cloud radiative properties. The identity of
83 INPs in the SML, and the factors governing their abundance, remain unknown.

84

85 In this work, low mass resolution liquid chromatography mass spectrometry was used
86 to explore the molecular composition of dissolved organic matter (DOM) isolated
87 from Arctic SML and underlying seawater, with the aim of identifying features which
88 related to ice nucleation activity, an atmospherically relevant property. A combination
89 of high-mass resolution mass spectrometric techniques was then used to examine
90 these features further. The work was conducted as part of the Aerosol-Cloud Coupling
91 and Climate Interactions in the Arctic (ACCACIA) project.

92 **Experimental section**

93

94 **Sample collection**

95 Samples were collected from the Greenland and Barents Seas during cruise JR288 of
96 the RRS *James Clark Ross* in July-August 2013. Water sampling locations are shown
97 in Figure 1 and further details are given in Table S1 of Supplementary Information
98 (SI). Sea surface microlayer samples were collected using a remote controlled rotating
99 drum type sampler deployed for approximately 40 minutes per sample^{29, 39}. Sub-
100 samples of ~1 L were taken for mass spectrometric analysis. Two sampling blanks
101 ('boat blanks') were collected by running underlying seawater from the same location
102 over the sampler drum, and consequently through the sampler's whole collection
103 system. Underlying seawater was collected from approximately 2-5 m depth using
104 Niskin bottles deployed on a CTD rosette. Seawater subsamples (~10 L) were
105 collected from the Niskin bottles into dedicated clean glass sampling bottles that were
106 rinsed with dilute HCl (10% v/v) prior to the start of the cruise.

107

108 Atmospheric aerosol samples were collected during cruise JR288, and also during a
109 cruise to the same area made by the RV *Lance* in March 2013. Aerosol samples were
110 collected onto pre-combusted quartz (Whatman QM-A) filters using a high volume
111 aerosol collector (Ecotech Hi-vol 3000; air flow ~68 m³ hr⁻¹) fitted with a PM_{2.5} size
112 selective inlet. The sampler was located on the bridge-top deck of each ship, and
113 automatically controlled according to wind direction in order to avoid contamination
114 from the ship's stack. Individual samples were collected over 24 hour periods, with an
115 average total air volume of 1261 m³ per sample.

116

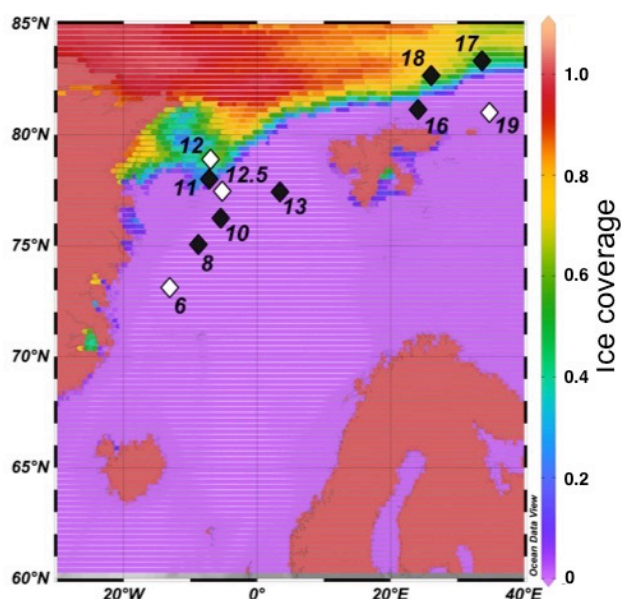


Figure 1. Locations of sea surface microlayer sampling stations during cruise JR288, superimposed on NSIDC satellite sea ice concentration data for 28 July 2013. Sea ice concentrations are shown as fractional coverage, where 0 is no ice and 1 is complete cover; values >1 are masks for land and missing data. White station symbols indicate locations where the microlayer had particularly high relative ice nucleation activity, based on median freezing temperatures, T_{50} . Figure produced using Ocean data View⁴⁰.

Sample preparation

Immediately following collection, all seawater and microlayer samples were filtered under vacuum through pre-combusted (5 hours at 450°C) Whatman GF/F filters (nominal pore size 0.7 μm). Dedicated acid washed glass bottles and a polycarbonate filter holder were used; all were acid rinsed at least every few days. Dissolved organic matter was isolated from the filtrate by solid phase extraction (SPE) onto Agilent

136 Bond Elut PPL cartridges, using LC-MS grade solvents (Fisher Optima), according to
137 the method of Dittmar et al⁴¹. Procedural blanks were prepared by replacing the
138 sample with ~5 mL of rinse solution (0.01M hydrochloric acid). The operationally
139 defined fraction of the DOM isolated by this procedure is referred to as SPE-DOM.
140 SPE extraction efficiency was not evaluated here, but a previous comparison of
141 sorbents found the protocol adopted here to be the most efficient at extracting DOM
142 from seawater, with average recoveries of 43 and 62% for coastal and open ocean
143 waters respectively⁴¹. Longnecker et al⁴² achieved DOM recoveries from Arctic
144 seawater of 32 to 43% using a variation of this method with two SPE extraction steps.
145
146 Methanolic extracts were stored in pre-combusted glass vials at -20 °C for return to
147 the UK. Prior to analysis, samples were evaporated to dryness using a vacuum solvent
148 evaporator (Biotage, Sweden) and redissolved in methanol-water (1:1 mixture).
149 Potential exists for organic matter to undergo molecular transformations, such as
150 trans-esterification of carboxylic acids and esters⁴³, and acetal and hemi-acetal
151 formation⁴⁴, in methanolic extracts. Some of these changes may occur very rapidly,
152 over timescales of minutes, and so be effectively unavoidable. During longer-term
153 storage, it has been shown that methanolic extracts may undergo proton exchange but
154 not esterification or hemiacetal formation⁴⁵. Repeat analyses of our samples after
155 more than 12 months also suggests they are stable at -20 °C.
156
157 Aerosol samples were foil wrapped and frozen at -20°C immediately following
158 collection for return to the UK. Aerosol material was extracted from the filters into
159 ultrapure water (Fisher LC-MS grade) by ultrasonication, and then extracted by SPE
160 as above. To allow direct comparison of seawater and aerosol SPE-DOM, the salinity

161 of the aqueous aerosol extracts was made up to that of seawater ($\sim 35 \text{ g L}^{-1}$) by adding
162 sodium chloride prior to SPE. As aerosol loadings were very low, extracts from three
163 or four consecutive aerosol samples of the same air mass origin (assigned using air
164 mass back trajectories from NOAA Hysplit ⁴⁶) were combined.

165

166 **Mass spectrometric analysis**

167

168 *High performance liquid chromatography-ion trap mass spectrometry (LC-IT-MS).*

169 The SPE-DOM sample extracts were first analyzed by LC-IT-MS using an HCT Plus
170 ion trap mass spectrometer (Bruker Daltonics GmbH, Bremen, Germany) coupled to
171 an Agilent 1100 series HPLC. A Pinnacle DB-C₁₈ column with 5 μm particle size
172 (Restek, 4.6 x 150 mm) was used with 0.1% (v/v) formic acid in ultrapure water
173 (Optima LC-MS grade, Fisher, UK) and methanol (Optima LC-MS grade, Fisher,
174 UK) mobile phases and a flow rate of 0.6 mL min^{-1} . Gradient elution was performed
175 as follows: 0-13 minutes 20% methanol; 13-23 minutes increase to 60% methanol;
176 23-33 minutes, hold at 60% methanol; 33-43 minutes increase to 100% methanol; 43-
177 50 minutes hold at 100% methanol; 50-53 minutes return to starting conditions; 53-59
178 minutes hold at starting conditions. Electrospray ionization was used with a source
179 temperature of 365°C , nebulizer pressure of 70 psi and drying gas (N_2) flow rate of 12
180 L min^{-1} . The mass spectrometer was operated in alternating positive and negative ion
181 mode, with a scan range of m/z 50 - 1000 and a target mass setting of m/z 150. Mass
182 calibration was conducted using a standard containing arginine clusters (Sigma-
183 Aldrich). The mass accuracy ranged from ~ 100 to 2000 ppm, and the mass resolution
184 was 500 at m/z 200.

185

186 *Fourier transform ion cyclotron resonance mass spectrometry (FT-ICR-MS).* SPE-
187 DOM extracts were also analyzed by ultra-high mass resolution FT-ICR-MS with
188 electrospray ionization using a Solarix XR 9.4T instrument (Bruker Daltonics,
189 Coventry, UK). Samples were introduced by direct infusion at a flow rate of
190 120 $\mu\text{L hr}^{-1}$. The source temperature was 220 $^{\circ}\text{C}$, the nebulizer gas (N_2) pressure was
191 1.2 bar and the drying gas flow rate was 4 L min^{-1} . Samples were analyzed separately
192 in positive and negative mode over a scan range of m/z 58 to 1200. Each sample was
193 analyzed twice, typically with 50 (negative mode) or 200 (positive mode) scans
194 collected per analysis. The mass resolution was $\sim 140,000$ at m/z 200. The instrument
195 was externally calibrated using sodium formate clusters. Negative mode FT-ICR-MS
196 spectra were internally recalibrated using the ubiquitous series of DOM anions
197 ($\text{C}_{17}\text{H}_{19}\text{O}_8^-$, $\text{C}_{18}\text{H}_{21}\text{O}_8^-$, $\text{C}_{19}\text{H}_{23}\text{O}_8^-$ etc) proposed by Kujawinski et al., 2009⁴⁷. Positive
198 mode FT-ICR-MS spectra were internally calibrated using a combination of DOM
199 and common contaminant ions (e.g. proline, arginine, polyethylene glycol oligomers).
200 Aerosol SPE extracts were screened for selected ions using FT-ICR-MS in negative
201 mode, with conditions as above. Due to a lack of suitable ions, internal mass
202 calibration was not carried out for these samples.

203

204 Bulk compositional analysis was conducted for FT-ICR-MS data collected in the
205 negative mode, as this has been more widely reported in comparable previous studies.
206 Only m/z values that satisfied the following criteria were considered: (i) absent from
207 the procedural extraction blank (at a signal to noise ratio of at least four); (ii) present
208 in both analytical replicates; (iii) signal-to-noise ratio greater than ten. Molecular
209 formulae were generated using the SmartFormula functionality within DataAnalysis
210 4.1 software (Bruker Daltonics, Bremen, Germany), In addition to C, H and O, the

heteroatoms N, S and P were allowed, with a formula error limit of 1 ppm. Elemental combinations were restricted according to rules adopted from similar previous work^{22, 48-54}, see SI for further details.

High-performance liquid chromatography - quadrupole time-of-flight mass spectrometry (LC-TOF-MS²). A subset of microlayer and seawater extracts were analyzed by LC-TOF-MS² using a maXis 3G mass spectrometer (Bruker Daltonics, Coventry, UK) coupled to a Dionex ultimate 3000 HPLC system (Thermo Scientific Inc., UK). The column, mobile phases and gradient program were the same as those used for LC-IT-MS analysis (see above), with the exception that HPLC grade water (Fisher, UK) was used instead of LC-MS grade water. Differences in instrument plumbing resulted in a slight retardation of retention times of ~2 minutes. Electrospray ionization was used with a source temperature of 350°C, nebulizer pressure of 4 bar and drying gas (N₂) flow rate of 9 L min⁻¹. Samples were analyzed in positive and negative mode separately; in each mode external mass calibration was conducted using Agilent low concentration tuning mix (part no. G1969-85000). Fragmentation spectra for specified ions were acquired across a range of collision energies (7-40 eV) in order to obtain good fragmentation spectra for as many ions as possible.

The purpose of the LC-TOF-MS² analysis was to allow high confidence assignment of molecular formulae to selected ions of interest identified by LC-IT-MS. This was achieved in two ways. Firstly, it provided more accurate m/z values for ions of interest for which the retention time was known, so constrained the number of corresponding peaks in the FT-ICR-MS spectra. FT-ICR-MS spectra of microlayer samples,

236 seawater samples and procedural blanks within this narrower m/z window were then
237 compared to identify ions present at appropriate relative abundances, and possible
238 molecular formulae for these were generated. Secondly, possible formulae for
239 fragment ions and constant neutral losses detected by LC-TOF-MS² were used to
240 identify relationships between groups of ions and inform formula selection. This
241 information was combined with the FT-ICR-MS results in order to deduce probable
242 molecular formulae for the target ions.

243

244 **Supporting parameters**

245 The measurement of ice nucleating particles (INP) in untreated SML samples is
246 described in Wilson et al., 2015. In order to determine whether INP were retained
247 during the SPE extraction (Section 2.2), INP assays were also conducted on SML
248 extracts that had been dried and reconstituted in a salt-water matrix (35 g L⁻¹) and a
249 matrix blank. The reconstitution volume was selected such that analyte concentrations
250 were returned to those in the original, untreated SML sample. This allowed direct
251 comparison of the extract IN activity with the microlayer IN activity measured in the
252 raw samples during cruise JR288²⁹.

253

254 Total organic carbon content of untreated SML samples was measured using a
255 Shimadzu TOC-V analyzer, as described in Wilson et al., 2015. A suite of trace gases
256 (DMS, halocarbons, monoterpenes) were measured by purge-and-trap gas
257 chromatography mass spectrometry using the method described in⁵⁵, though we
258 caution that these results are semi-quantitative at best because microlayer sampling
259 methods were not gas-tight.

260

261 **Results and discussion**

262

263 **Presence of microlayer enhanced ions revealed by LC-IT-MS**

264 Low mass resolution LC-IT-MS analysis of all samples revealed differences in
265 organic composition, both between seawater and microlayer extracts, and within the
266 subset of microlayer extracts. Total ion chromatograms obtained using LC-IT-MS
267 showed a broad peak between 18 and 36 minutes in seawater and microlayer samples,
268 while procedural blanks did not (Figs S1a, S2a). This broad peak is thought to be due
269 to a large number of co-eluting, organic compounds present at low concentrations⁵⁶.
270 For some, but not all microlayer samples, discrete peaks appeared superimposed upon
271 the broader hump (Figs S1a, S2a), suggesting a small number of ions either present at
272 elevated levels, or with substantially higher ionization efficiencies. Base peak
273 chromatograms (which display the abundance of the most intense ion in the mass
274 spectra at each time point) confirmed the enhancement of selected ions in the
275 microlayer (Figs S1b, S2b). In contrast, seawater samples did not exhibit any discrete
276 peaks within this region.

277

278 Average mass spectra calculated for the 18-36 minute retention time region showed a
279 characteristic distribution of peaks separated by 14 Da (corresponding to a CH₂ unit)
280 for all seawater samples (Fig S3). Note that the choice of instrumental parameters
281 (e.g. target mass) will influence the shape and center of the m/z distributions obtained,
282 as well as the response factors of individual ions, so only data obtained under the
283 same conditions can be directly compared. Average mass spectra were strikingly
284 similar for all seawater samples, suggesting homogeneity in the extracted organic
285 matter between sampling stations. Average mass spectra of microlayer samples

286 displayed additional peaks with higher relative intensity than observed in the seawater
287 samples (Fig S3). This is consistent with the presence of elevated concentrations of
288 certain ions in the microlayer compared to the underlying seawater.

289

290 LC-IT-MS chromatograms for microlayer sampling boat blanks did not contain these
291 enhanced species, and the average mass spectra appeared similar to those for the
292 seawater from which they were prepared (Figs S1, S2 and S3), suggesting they were
293 not the result of contamination during microlayer sampling.

294

295 Inspection of base peak chromatograms and average mass spectra obtained by LT-IT-
296 MS found 33 negative ions and 117 positive ions that were enhanced in microlayer
297 samples, and these ions were selected for further study. Peak areas (obtained from
298 extracted ion chromatograms) for these microlayer enhanced ions were normalized
299 according to aqueous extraction volume, and used as a proxy for their relative
300 abundances. As the sensitivity of ESI-MS varies across different compounds and as a
301 function of matrix, peak areas are only used to compare the same ions (at same
302 retention time and so approximately same matrix) across samples, and not to compare
303 abundances of different ions within or between samples.

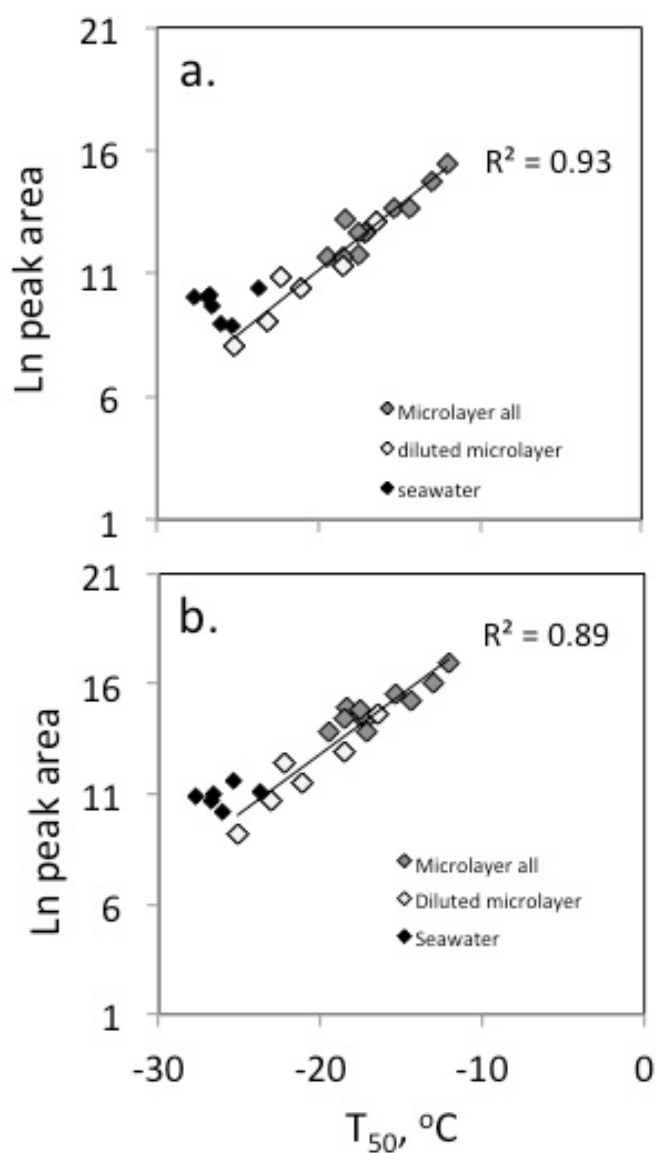
304

305 **Link between abundance of microlayer enhanced ions and ice nucleation activity**

306 The microlayer samples had higher ice nucleation (IN) activity than the underlying
307 seawater, and this varied between stations (see Wilson et al., 2015). Ice nucleation
308 ability, quantified in terms of median freezing temperature (T_{50} ; the temperature at
309 which 50% of droplets had frozen), was correlated with the relative abundances of
310 some of the microlayer enhanced ions identified by LC-IT-MS analysis (Fig 2, Table

311 1). Considering the microlayer samples only, linear correlation coefficients of $R^2 >$
312 0.5 were obtained for 7 negative ions and 27 positive ions (Table 1); for ease, these
313 ions are referred to as 'IN tracer ions' hereafter. To examine this relationship over a
314 wider linear range, correlation analysis was extended to include the measured IN
315 activity of diluted microlayer samples (1% and 10% by volume) and calculated ion
316 abundance, assuming that peak area scales linearly for the ions of interest. This
317 revealed strong exponential relationships between IN activity and IN tracer ion
318 relative abundance, with correlation coefficients of $R^2 > 0.8$ in all but one case (Fig 2,
319 Table 1). Seawater samples also appear to broadly fit this relationship (Fig 2), but
320 were not included in quantitative correlation analysis as both ice nucleation ability
321 and peak area were at or very close to the limit of detection.

322



323

324

325 **Figure 2.** Natural log of volume normalized peak area plotted against 50% freezing
 326 temperature, for ions with (a) retention time 30.8 mins, $[M-H]^- = 289.2$ and (b)
 327 retention time 38.5 mins, $[M+H]^+ = 285.2$ for microlayer (grey diamonds) and
 328 seawater (black diamonds) samples, and microlayer samples diluted with ultrapure
 329 water to 10 and 1% by volume (white diamonds). Lines of best fit and correlation
 330 coefficients are for microlayer (whole and diluted) only, assuming peak area scales

331 linearly with sample dilution; seawater values were excluded from correlation
332 analysis as they were at or close to the limit of detection for both ice nucleation ability
333 and peak area.

334

335 The correlations between IN tracer ion abundance and T_{50} for microlayer samples are
336 comparable or greater than that identified between T_{50} and TOC content of the
337 microlayer ($R^2 = 0.51$). For many ions, the relationship between ion abundance and
338 IN activity was also stronger than that between ion abundance and TOC (Table 1).
339 The IN tracer ions were variably correlated with TOC (Table 1), consistent with
340 compositional differences between the SML samples, rather than solely a
341 homogenous DOC pool present at varying concentrations.

342

343 IN assays of reconstituted SPE extracts yielded freezing curves that were very similar
344 to those of the salt-water matrix (Fig. S4) and of the fresh seawater analyzed
345 immediately following collection²⁹. The elevated freezing temperatures characteristic
346 of the raw microlayer samples²⁹ were not observed in the reconstituted SPE extracts.
347 This implies that the INPs are not extracted and/or preserved by the SPE protocol, and
348 that the IN tracer ions are only associated with INPs, but do not contribute directly to
349 ice nucleation.

350

351

352

353

354

355 **Table 1.** Formula assignment, correlation coefficients (R^2) and enrichment factors (EF) for ice nucleation tracer ions that were enhanced the
356 SML, in order of retention time (t_R).

t_R , mins	Mode	Exact m/z	Suggested formula	Formula error, ppm	Adduct	Fragment ions	R^2 Peak area vs. T_{50}	R^2 Ln(peak area) vs. T_{50}^*	R^2 Peak area vs. TOC	EF range
23.1	+	187.09647	$C_9H_{14}O_4$	0.08	$[M+H]^+$	b	0.56	0.87	0.62	12 - 436
23.9	+	273.13086	$C_{11}H_{22}O_6$	-0.00	$[M+Na]^+$	a	0.52	0.85	0.56	16 - 85
24.3	+	197.11723	$C_{11}H_{16}O_3$	-0.05	$[M+H]^+$	179.11, 161.10, (135), 133.10, 107.09, 93.07	0.55	0.84	0.85	29 - 1502
26.5	-	261.13429	$C_{12}H_{22}O_6$	-0.27	$[M-H]^-$	187.09, 125.09	0.52	0.85	0.52	2 - 175
28.6	+	285.13105 285.16727	$C_{12}H_{22}O_6$ $C_{13}H_{26}O_5$ $C_{19}H_{25}S^+$	-0.65 -0.09 -0.43	$[M+Na]^+$ $[M+Na]^+$	a	0.58	0.81	0.26	8 - 167
29.4	+	125.09606	$C_8H_{12}O$	0.25	$[M+H]^+$	a	0.61	0.90	0.55	6 - 97
29.7	+	299.14675	$C_{13}H_{24}O_6$	-0.80	$[M+Na]^+$	73.6079	0.56	0.80	0.26	14 - 101
29.9	+	123.11685	C_9H_{14}	-0.19	$[M+H]^+$	b	0.58	0.81	0.46	18 - 124

30.7	+	273.13086	C ₁₁ H ₂₂ O ₆	0.00	[M+Na] ⁺	c	0.58	0.86	0.48	6 - 50
		273.16968	C ₁₄ H ₂₄ O ₅	-0.11	[M+H] ⁺					
30.8	-	289.15757	C ₁₄ H ₂₇ O ₄ P	0.61	[M-H] ⁻	215.12	0.71	0.93	0.50	5 - 115
		289.16557	C ₁₄ H ₂₆ O ₆	-0.31	[M-H] ⁻					
31.0	+	315.17790	C ₁₄ H ₂₈ O ₆	-0.30	[M+Na] ⁺	a	0.52	0.81	0.42	28 - 272
31.5	-	187.13382	C ₁₀ H ₂₀ O ₃	-0.46	[M-H] ⁻	167.10, 151.04, 141.12, 112.98	0.56	0.87	0.53	35 - 647
31.6	+	171.13797	C ₁₀ H ₁₈ O ₂	-0.08	[M+H] ⁺	153.13, 135.12, 107.09	0.55	0.86	0.54	12 - 266
31.7	+	273.16968	C ₁₄ H ₂₄ O ₅	-0.11	[M+H] ⁺	153.13, 135.12	0.57	0.81	0.39	11 - 399
31.8	-	289.15757	C ₁₄ H ₂₇ O ₄ P	0.61	[M-H] ⁻	215.12, 197.11	0.61	0.86	0.46	23 - 894
		289.16557	C ₁₄ H ₂₆ O ₆	-0.31	[M-H] ⁻					
31.9	+	257.17489	C ₁₄ H ₂₄ O ₄	-0.60	[M+H] ⁺	211.08, 147.12, 137.13, 95.09	0.52	0.82	0.60	3 - 326
33.9	+	187.13281	C ₁₀ H ₁₈ O ₃	0.33	[M+H] ⁺	173.12, 155.11, 137.10, 119.09, 109.10, 95.09	0.53	0.86	0.57	41 - 744
34.0	+	241.14100	C ₁₁ H ₂₂ O ₄	-0.12	[M+Na] ⁺	209.12	0.54	0.81	0.41	82 - 1952
35.7	+	241.14100	C ₁₁ H ₂₂ O ₄	0.12	[M+Na] ⁺	209.12	0.58	0.85	0.68	15 - 273
36.6	+	167.14304	C ₁₁ H ₁₈ O	0.19	[M+H] ⁺	149.13, 121.10, 109.10, 95.09, 81.07	0.57	0.87	0.72	162 -

										5512
36.7	-	201.14952	C ₁₁ H ₂₂ O ₃	0.49	[M-H] ⁻	155.14	0.55	0.87	0.69	386 - 12931
36.7	+	149.13246	C ₁₁ H ₁₆	0.11	[M+H] ⁺	121.10, 109.10, 107.09, 95.09	0.56	0.87	0.69	17 - 625
36.7	+	185.15361	C ₁₁ H ₂₀ O ₂	-0.02	[M+H] ⁺	167.14, 149.13, 121.10, 109.10, 95.09, 83.09, 81.07	0.56	0.87	0.71	86 - 1927
38.5	+	285.20581	C ₁₆ H ₂₈ O ₄	0.79	[M+H] ⁺	b	0.66	0.89	0.53	17-67
39.1	+	125.13251	C ₉ H ₁₆	-0.26	[M+H] ⁺	c	0.52	0.87	0.67	9 - 114
39.2	-	236.11384	C ₂₀ H ₄₂ O ₈ S ₂	-0.85	[M-2H] ²⁻	375.24, 96.96	0.64	0.84	0.29	52 - 1944
40.1	-	236.11384	C ₂₀ H ₄₂ O ₈ S ₂	-0.85	[M-2H] ²⁻	375.24, 195.13, 154.06, 96.96	0.64	0.78	0.16	25 - 3728
40.7	+	257.17464	C ₁₄ H ₂₄ O ₄	-0.37	[M+H] ⁺	201.15, 183.14, 165.13, 147.12, 137.13, 123.12, 95.09	0.53	0.84	0.49	8 - 244

357 Where two different m/z are listed, it was not possible to unambiguously identify the tracer ion in the FT-ICR-MS spectra. Where fragment ions
358 are not given either (a) the ion did not fragment, (b) the fragmentation spectra were of very low intensity, or (c) the tracer ion was not apparent in
359 the LC-TOF-MS² chromatogram. Rows shaded grey indicate formulae that are related to each other by the loss or gain of water molecules, so
360 may indicate adducts of the same compound. Correlation coefficients are shown for relative abundance versus ice nucleation ability, measured as
361 median freezing temperature (T_{50}), and total organic carbon content (TOC). *Correlation of $\ln(\text{peak area})$ against T_{50} includes diluted microlayer

362 samples. Enrichment factors are estimated as the ratio of the peak area in a microlayer sample to that in the corresponding seawater sample,
363 following adjustment for extraction volume; the range for all microlayer samples is shown.

364 **Identity and potential origin of IN tracer ions**

365 Microlayer enhanced peaks (and high IN activity) were particularly common and
366 abundant at station 12, and also stations 6, 12.5 and 19 (Figs S1, S2 and S3). The
367 underlying water at stations 6, 12, 12.5 and 19 did not exhibit any distinctive features
368 in either total or size-segregated chlorophyll concentrations (C. Hughes, University of
369 York, unpub. data), or the chlorophyll contribution of individual phytoplankton
370 groups derived from pigment analysis (A. Small, Oxford University, unpub. data).
371 Similarly, there was no apparent relationship between the variation in SML
372 composition (as determined here) or freezing temperature (as presented in Wilson et
373 al.²⁹) and the numbers of bacteria present (cell count data presented in Wilson et al.²⁹).
374 Examination of temperature-salinity profiles, and the shipboard wind speed and
375 ambient light levels at the time of sampling, and in the 6 and 24 hours prior to the
376 SML sampling, also failed to show any corresponding trends. Interestingly, semi-
377 quantitative determinations of the biogenic trace gases dimethyl sulfide, methyl
378 iodide, bromochloromethane and di-iodomethane revealed that these gases also
379 tended to be present at higher levels in microlayer samples 6, 12, 12.5 and 19 than in
380 other samples (Fig S5). These stations were also unusual in that ethyl and propyl
381 iodide were observed. From the above consideration of the available supporting
382 evidence, a single factor associated with the relative abundance of IN tracer ions (and
383 high INPs themselves) cannot be identified, but the associations with TOC and
384 biogenic trace gases point towards a biological and/or photochemical influence.

385

386 The nature of marine INPs has not yet been fully elucidated, but evidence suggests
387 they originate from marine phytoplankton or bacteria⁶⁰⁻⁶⁴. Phytoplankton cell exudates
388 and/or cellular fragments, and the bacterial populations sustained by this material,

389 have both been suggested as possible sources^{29, 36, 63}. Laboratory mesocosm
390 experiments found that peaks in airborne IN activity coincided with increases in
391 relatively aliphatic rich, low O/C organic material in submicron SSA; these changes
392 were ascribed to phytoplankton cell lysis under conditions of relatively low bacterial
393 lipase activity^{36, 64, 65}. Cell breakage may occur in the surface ocean, with subsequent
394 concentration of the products in the SML, or the process may be enhanced in the SML
395 itself. Enrichments of mannose and arabinose in the SML have previously been
396 attributed to phytoplankton cell degradation⁶⁶. Aller et al.⁶⁷ observed an increased
397 proportion of membrane damaged cells in the SML, and suggested this might be due
398 to the increased potential for viral infection, zooplankton grazing and physical
399 stresses in the microlayer. Either process could potentially result in increased
400 abundances of INPs and other biogenic material in the SML. We hypothesize that the
401 IN tracer ions originate from a phytoplankton exudate mix (including any associated
402 bacteria and viruses), of which larger sized constituents confer the IN activity.

403

404 Phytoplankton are known to release a wide variety of organic compounds, ranging in
405 size from volatile gases of less than 100 Da to macromolecules and colloids of several
406 1000 Da. As a result of sample processing and instrumental constraints, this study
407 (and all others using similar approaches), considers only an operationally defined
408 fraction of the total organic matter present. Specifically, the analytical approaches
409 used here have targeted compounds that are low molecular weight ($<1000\ m/z$), water
410 soluble, neither strongly hydrophobic or strongly hydrophilic, and easily ionizable by
411 electrospray. High-resolution mass spectrometry was used to elucidate molecular
412 formulae for the IN tracer ions (Table 1). Searches of online databases (e.g.
413 Chemspider, MassBank, NIST) typically returned tens of structural isomers per

414 formula or more. Our data is insufficient to distinguish between these isomers, so we
415 can only explore whether the IN formulae are consistent with algal exudates. For
416 example, known algal metabolites with similar carbon numbers to the IN tracer ions
417 include polyunsaturated aldehydes (PUAs; e.g. decatrienal, $C_{10}H_{14}O$)⁶⁸ and
418 unsaturated hydrocarbons (e.g. fucoserratene, C_8H_{12} ; dictyopterene, $C_{11}H_{18}$)⁶⁹. Two
419 tracer ion formulae exactly match those of compounds from these classes: isomers of
420 $C_8H_{12}O$ include the PUA octadienal, while those of $C_{11}H_{16}$ include the algal hormone
421 hormosirene⁷⁰. Other tracer ions have formulae consistent with oxygenated organics
422 (e.g. $C_8H_{14}O_3$, $C_{12}H_{16}O_3$) formed when PUAs are produced by the cleavage of higher
423 molecular weight polyunsaturated fatty acids (PUFA)⁷¹. PUAs are mainly produced
424 by diatoms, as a response to cell wounding, for example by zooplankton grazing⁷²;
425 the elevated levels of DMS (and potentially halocarbons) observed in the samples
426 with high levels of the IN tracer ions are indicative of grazing having taken place at
427 these locations⁷³. It is beyond the scope of this work to prove that the IN tracer ions
428 were indeed derived from PUAs, but we speculate that cellular damage (e.g. by
429 grazing, stress or viral infection) could cause the simultaneous release of PUAs, trace
430 gases and INPs.

431

432 The IN tracer ions were massively enriched in the SML, with enrichment factors
433 ranging from ~2 to 12931 (Table 1). Such EF values are several orders of magnitude
434 greater than observed for dissolved organic carbon and other organic molecules¹²,
435 supporting the possibility that the tracer ions were formed *in-situ*. One possible
436 mechanism for this is the photo-chemical modification of organic matter within the
437 SML. Many have formulae consistent with fatty acid and dicarboxylic acid groups,
438 e.g. saturated oxo-fatty acids ($C_nH_{2n-2}O_3$), and unsaturated dicarboxylic acids (C_nH_{2n-}

$_4\text{O}_4$), which have been tentatively identified in nascent sea spray aerosol⁷⁴. Compounds of these classes, including nine with identical formulae to the IN tracer ions, have been found to increase in abundance following the irradiation of cellular material from freshwater aquatic biofilms⁷⁵. More generally, the photochemical production of low molecular weight, saturated and unsaturated, carbonyl compounds has been demonstrated in natural microlayer samples and model systems^{4, 5, 16, 76}. Alternative oxidation mechanisms include the oxidation of unsaturated organic compounds by ozone at the air-sea interface⁷⁷, or bacterial metabolism in the SML^{1, 28}. Formation of the IN tracer ions within the SML by abiotic reactions or bacterial breakdown is not incompatible with a link to phytoplankton described above, as this may supply the precursor material.

Semi-quantitative comparison of seawater and microlayer SPE-DOM composition using FT-ICR-MS

Mass spectra obtained using the high resolution FT-ICR-MS echoed the general trends suggested by the LC-IT-MS analysis, described earlier. Seawater samples were similar across stations, even at the fine scale. The negative mode high-resolution mass spectra for seawater samples visually resemble those obtained in other studies^{22, 47, 57, 58}. As mentioned earlier, it should be noted that relative ion intensities across the m/z range scanned are in part a function of user selected instrument settings. Previous studies have also reported a high level of homogeneity between SPE-DOM mass spectra for surface seawater samples^{57, 58}.

In contrast, SML samples displayed differences both from seawater and each other, but boat blanks were very similar to those for seawater (Fig S6). The SML spectra

464 tended to contain peaks across a wider m/z range than the seawater spectra, and have
465 more high intensity spikes. In the negative mode, higher molecular weight peaks (m/z
466 ~ 700 to 900) were particularly prominent in SML samples 6 and 12.5, which also had
467 high IN activity.

468

469 The visual contrast between seawater and SML spectra resembles the differences
470 observed between ESI-FT-ICR mass spectra of underlying seawater and SML from an
471 estuary, where enhancement of surfactant peaks has been observed²². Interestingly,
472 seawater samples incubated with different microbial communities have also been
473 shown to exhibit comparable differences in low molecular weight DOM
474 composition⁵⁹. In that study, plankton larger than $\sim 1 \mu\text{m}$ were removed from
475 seawater, resulting in a microbial community dominated by heterotopic bacteria.
476 High-resolution mass spectra from these incubations revealed the presence of unique,
477 high-abundance ions that were not present in spectra from whole water, and overall
478 had higher average H/C ratios and lower DBE values⁵⁹. In light of these findings, it
479 seems plausible that differences in the DOM composition of the microlayer relative to
480 seawater observed here could, at least in part, reflect the differing microbial
481 communities in each.

482

483 In the positive mode LC-IT-MS average spectra, there is some indication that the
484 microlayer may be depleted in compounds at the higher molecular weight end of the
485 detection envelope (m/z 200-400; Fig S2) relative to seawater. This is in agreement
486 with the shift to smaller molecular size in the microlayer observed by Lechtenfeld et
487 al.²², which was attributed to photochemical and microbiological degradation.
488 Meanwhile, negative mode FT-ICR-MS spectra obtained by direct injection also

suggested the presence of additional higher molecular weight ($m/z \sim 700$ to 900) peaks in some SML samples that were absent from seawater (Fig S6). These peaks were not present in the LC-IT-MS average mass spectra (Supp info Fig S3A), probably because they have long retention times and did not elute in the time window of interest.

Assignment of molecular formulae to negatively charged ions detected by FT-ICR-MS is described in the SI. Formula assignment for complex organic mixtures, where multiple heteratoms must be considered, can be ambiguous^{78,79}, and we consider our results to be subject to uncertainty. Average DBE values and H/C ratios suggested SPE-DOM from the microlayer was slightly more aliphatic than that from seawater (Table S2). A tendency towards higher saturation and decreased aromaticity in the microlayer relative to the underlying seawater has been observed previously^{19,22}, and is consistent with the enhancement of hydrophobic substances in the microlayer. That the SML was more aliphatic than the underlying water, and also had higher IN activity, is consistent with the observation of an association between IN activity and more aliphatic material in SSA^{36,64,65}. However, we did not observe trends in average elemental ratios or DBE values within the SML subset that co-varied with IN activity.

Possible occurrence of SML derived compounds in atmospheric aerosol

The presence of relatively low molecular weight, highly oxygenated compounds in the sea surface microlayer, raises the possibility that primary sea spray aerosol may also contribute to the atmospheric aerosol burden of such compounds in the marine environment. FT-ICR-MS identified ions with the same molecular formulae as five of the negatively charged IN tracer ions (Table 1) in ambient atmospheric aerosol

514 sampled in the Greenland Sea during the July-August 2013, but not March 2013
515 (Table S3). Good agreement between observed spectra and simulated isotopic patterns
516 (indicated by a relatively low mSigma value) confirmed that the molecular formulae
517 agreed. These ions were absent from the aerosol sampling procedural blanks. The
518 possible occurrence of IN tracer ions in ambient atmospheric aerosol is consistent
519 with the transfer of material, possibly including INPs, from the microlayer to sea
520 spray aerosol. It has recently been demonstrated that SSA produced by wave breaking
521 contains INPs at levels in agreement with ambient INP measurements made over the
522 oceans³⁶. That the IN tracer ions were only found in aerosol collected during the
523 summer, and not the early spring, is consistent with a biological source for these ions.

524

525

526

527 **Acknowledgements**

528 We acknowledge funding from the NERC ACCACIA (Aerosol-Cloud Coupling And
529 Climate Interactions in the Arctic) project (NE/I028769/1), and are grateful to the
530 Principal Investigator Prof Ian Brooks and to the cast and crew of the R/V *Lance*
531 March 2013 and JR288 July 2013 cruises. The York Centre of Excellence in Mass
532 Spectrometry was created thanks to a major capital investment through Science City
533 York, supported by Yorkshire Forward with funds from the Northern Way Initiative.
534 We thank Ed Bergström and David Ashford for assistance with FT-ICR-MS and
535 maXis LT-TOF-MS² analyses respectively. The authors gratefully acknowledge the
536 NOAA Air Resources Laboratory (ARL) for the provision of the HYSPLIT transport
537 and dispersion model and/or READY website (<http://www.ready.noaa.gov>) used in
538 this publication.

539

Supporting information. The FT-ICR-MS formula assignment procedure is described in the SI. Table S1 contains microlayer (and seawater) sampling information, and Table S2 contains average elemental composition information derived from FT-ICR-MS analysis of these samples. Table S3 provides details of aerosol sample collection, air mass origin and presence/absence of IN tracer ions. Total ion and base peak chromatograms obtained by LC-IT-MS for all samples are shown in Figures S1 and S2, and average mass spectra from these analyses are compared in Figure S3. Figure S4 shows freezing curves for reconstituted microlayer extracts, and raw microlayer and seawater extracts. Figure S5 compares the relative abundance of selected IN tracer ions with approximate concentrations of trace gases in microlayer samples. Negative mode FT-ICR mass spectra for seawater, microlayer and procedural blanks are shown in Figure S6, numbers of molecular formulae found in each sample type are given in Figure S7 (Venn diagram), and Figure S8 is a van Krevelen plot of these results. This information is available free of charge via the Internet at <http://pubs.acs.org>.

References

1. Cunliffe, M.; Engel, A.; Frka, S.; Gasparovic, B.; Guitart, C.; Murrell, J. C.; Salter, M.; Stolle, C.; Upstill-Goddard, R.; Wurl, O. Sea surface microlayers: A unified physicochemical and biological perspective of the air-ocean interface. *Prog. Oceanogr.* **2013**, *109*, 104-116.
2. Wurl, O.; Wurl, E.; Miller, L.; Johnson, K.; Vagle, S. Formation and global distribution of sea-surface microlayers. *Biogeosciences* **2011**, *8* (1), 121-135.
3. Sabbaghzadeh, B.; Upstill-Goddard, R. C.; Beale, R.; Pereira, R.; Nightingale, P. D. The Atlantic Ocean surface microlayer from 50 degrees N to 50 degrees S is ubiquitously enriched in surfactants at wind speeds up to 13ms(-1). *Geophys. Res. Lett.* **2017**, *44* (6), 2852-2858.
4. Ciuraru, R.; Fine, L.; van Pinxteren, M.; D'Anna, B.; Herrmann, H.; George, C. Unravelling New Processes at Interfaces: Photochemical Isoprene Production at the Sea Surface. *Environ. Sci. Technol.* **2015**, *49* (22), 13199-13205.

- 572 5. Ciuraru, R.; Fine, L.; van Pinxteren, M.; D'Anna, B.; Herrmann, H.; George,
573 C. Photosensitized production of functionalized and unsaturated organic
574 compounds at the air-sea interface. *Scientific Reports* **2015**, *5*.
- 575 6. Ebling, A. M.; Landing, W. M. Sampling and analysis of the sea surface
576 microlayer for dissolved and particulate trace elements. *Mar. Chem.* **2015**, *177*,
577 134-142.
- 578 7. Shaw, M. D.; Carpenter, L. J. Modification of Ozone Deposition and I-2
579 Emissions at the Air-Aqueous Interface by Dissolved Organic Carbon of Marine
580 Origin. *Environ. Sci. Technol.* **2013**, *47* (19), 10947-10954.
- 581 8. del Vento, S.; Dachs, J. Influence of the surface microlayer on atmospheric
582 deposition of aerosols and polycyclic aromatic hydrocarbons. *Atmos. Environ.*
583 **2007**, *41* (23), 4920-4930.
- 584 9. Frew, N. M.; Bock, E. J.; Schimpf, U.; Hara, T.; Haussecker, H.; Edson, J. B.;
585 McGillis, W. R.; Nelson, R. K.; McKenna, S. P.; Uz, B. M.; Jahne, B. Air-sea gas
586 transfer: Its dependence on wind stress, small-scale roughness, and surface films.
587 *J. Geophys. Res.: Oceans* **2004**, *109* (C8), 23.
- 588 10. Donaldson, D. J.; George, C. Sea-Surface Chemistry and Its Impact on the
589 Marine Boundary Layer. *Environ. Sci. Technol.* **2012**, *46* (19), 10385-10389.
- 590 11. Blanchard, D. C. Sea-to-air transport of surface active material. *Science*
591 **1964**, *146* (364), 396-&.
- 592 12. Quinn, P. K.; Collins, D. B.; Grassian, V. H.; Prather, K. A.; Bates, T. S.
593 Chemistry and Related Properties of Freshly Emitted Sea Spray Aerosol. *Chem.*
594 *Rev.* **2015**, *115* (10), 4383-4399.
- 595 13. Leck, C.; Bigg, E. K. Biogenic particles in the surface microlayer and
596 overlaying atmosphere in the central Arctic Ocean during summer. *Tellus Series*
597 *B-Chemical and Physical Meteorology* **2005**, *57* (4), 305-316.
- 598 14. Roslan, R. N.; Hanif, N. M.; Othman, M. R.; Azmi, W.; Yan, X. X.; Ali, M. M.;
599 Mohamed, C. A. R.; Latif, M. T. Surfactants in the sea-surface microlayer and their
600 contribution to atmospheric aerosols around coastal areas of the Malaysian
601 peninsula. *Marine Pollution Bulletin* **2010**, *60* (9), 1584-1590.
- 602 15. Mungall, E. L.; Abbatt, J. P. D.; Wentzell, J. J. B.; Lee, A. K. Y.; Thomas, J. L.;
603 Blais, M.; Gosselin, M.; Miller, L. A.; Papakyriakou, T.; Willis, M. D.; Liggio, J.
604 Microlayer source of oxygenated volatile organic compounds in the summertime
605 marine Arctic boundary layer. *Proc. Natl. Acad. Sci. U.S.A.* **2017**, *114* (24), 6203-
606 6208.
- 607 16. Zhou, X. L.; Mopper, K. Photochemical production of low-molecular-
608 weight carbonyl compounds in seawater and surface microlayer and their air-sea
609 exchange. *Mar. Chem.* **1997**, *56* (3-4), 201-213.
- 610 17. van Pinxteren, M.; Muller, C.; Iinuma, Y.; Stolle, C.; Herrmann, H. Chemical
611 Characterization of Dissolved Organic Compounds from Coastal Sea Surface
612 Micro layers (Baltic Sea, Germany). *Environ. Sci. Technol.* **2012**, *46* (19), 10455-
613 10462.
- 614 18. Antonowicz, J. P. Daily cycle of variability contents of phosphorus forms in
615 surface microlayer of a light salinity Baltic Sea Lagoon lake (North Poland) - Part
616 II. *Central European Journal of Chemistry* **2013**, *11* (5), 817-826.
- 617 19. Calace, N.; Mirante, S.; Petronio, B. M.; Pietroletti, M.; Rugo, C. Fulvic acid
618 enrichment in the microlayer of the Gerlache Inlet sea (Antarctica): Preliminary
619 results. *International Journal of Environmental Analytical Chemistry* **2004**, *84* (6-
620 7), 413-421.

20. Garcia-Flor, N.; Guitart, C.; Abalos, M.; Dachs, J.; Bayona, J. M.; Albaiges, J. Enrichment of organochlorine contaminants in the sea surface microlayer: An organic carbon-driven process. *Mar. Chem.* **2005**, *96* (3-4), 331-345.
21. Hardy, J. T.; Cleary, J. Surface microlayer contamination and toxicity in the German Bight. *Mar. Ecol. Prog. Ser.* **1992**, *91* (1-3), 203-210.
22. Lechtenfeld, O. J.; Koch, B. P.; Gasparovic, B.; Frka, S.; Witt, M.; Kattner, G. The influence of salinity on the molecular and optical properties of surface microlayers in a karstic estuary. *Mar. Chem.* **2013**, *150*, 25-38.
23. Galgani, L.; Piontek, J.; Engel, A. Biopolymers form a gelatinous microlayer at the air-sea interface when Arctic sea ice melts. *Scientific Reports* **2016**, *6*, 10.
24. Cincinelli, A.; Stortini, A. M.; Perugini, M.; Checchini, L.; Lepri, L. Organic pollutants in sea-surface microlayer and aerosol in the coastal environment of Leghorn - (Tyrrhenian Sea). *Mar. Chem.* **2001**, *76* (1-2), 77-98.
25. Jayarathne, T.; Sultana, C. M.; Lee, C.; Malfatti, F.; Cox, J. L.; Pendergraft, M. A.; Moore, K. A.; Azam, F.; Tivanski, A. V.; Cappa, C. D.; Bertram, T. H.; Grassian, V. H.; Prather, K. A.; Stone, E. A. Enrichment of Saccharides and Divalent Cations in Sea Spray Aerosol During Two Phytoplankton Blooms. *Environ. Sci. Technol.* **2016**, *50* (21), 11511-11520.
26. Gao, Q.; Leck, C.; Rauschenberg, C.; Matrai, P. A. On the chemical dynamics of extracellular polysaccharides in the high Arctic surface microlayer. *Ocean Science* **2012**, *8* (4), 401-418.
27. Kuznetsova, M.; Lee, C.; Aller, J. Characterization of the proteinaceous matter in marine aerosols. *Mar. Chem.* **2005**, *96* (3-4), 359-377.
28. Kuznetsova, M.; Lee, C. Enhanced extracellular enzymatic peptide hydrolysis in the sea-surface microlayer. *Mar. Chem.* **2001**, *73* (3-4), 319-332.
29. Wilson, T. W.; Ladino, L. A.; Alpert, P. A.; Breckels, M. N.; Brooks, I. M.; Browse, J.; Burrows, S. M.; Carslaw, K. S.; Huffman, J. A.; Judd, C.; Kilhau, W. P.; Mason, R. H.; McFiggans, G.; Miller, L. A.; Najera, J. J.; Polishchuk, E.; Rae, S.; Schiller, C. L.; Si, M.; Temprado, J. V.; Whale, T. F.; Wong, J. P. S.; Wurl, O.; Yakobi-Hancock, J. D.; Abbatt, J. P. D.; Aller, J. Y.; Bertram, A. K.; Knopf, D. A.; Murray, B. J. A marine biogenic source of atmospheric ice-nucleating particles. *Nature* **2015**, *525* (7568), 234-.
30. Bigg, E. K. Ice nucleus concentrations in remote areas. *Journal of the Atmospheric Sciences* **1973**, *30* (6), 1153-1157.
31. Bigg, E. K. Ice forming nuclei in the high Arctic. *Tellus Series B-Chemical and Physical Meteorology* **1996**, *48* (2), 223-233.
32. Schnell, R. C. Ice nuclei in seawater, fog water and marine air off the coast of Nova-Scotia - summer 1975. *Journal of the Atmospheric Sciences* **1977**, *34* (8), 1299-1305.
33. Schnell, R. C.; Vali, G. Freezing nuclei in marine waters. *Tellus* **1975**, *27* (3), 321-323.
34. Schnell, R. C.; Vali, G. Biogenic ice nuclei. 1. Terrestrial and marine sources. *Journal of the Atmospheric Sciences* **1976**, *33* (8), 1554-1564.
35. Rosinski, J.; Haagenson, P. L.; Nagamoto, C. T.; Parungo, F. Nature of ice-forming nuclei in marine air masses. *Journal of Aerosol Science* **1987**, *18* (3), 291-.
36. DeMott, P. J.; Hill, T. C. J.; McCluskey, C. S.; Prather, K. A.; Collins, D. B.; Sullivan, R. C.; Ruppel, M. J.; Mason, R. H.; Irish, V. E.; Lee, T.; Hwang, C. Y.; Rhee, T. S.; Snider, J. R.; McMeeking, G. R.; Dhaniyala, S.; Lewis, E. R.; Wentzell, J. J. B.

Abbatt, J.; Lee, C.; Sultana, C. M.; Ault, A. P.; Axson, J. L.; Martinez, M. D.; Venero, I.; Santos-Figueroa, G.; Stokes, M. D.; Deane, G. B.; Mayol-Bracero, O. L.; Grassian, V. H.; Bertram, T. H.; Bertram, A. K.; Moffett, B. F.; Franc, G. D. Sea spray aerosol as a unique source of ice nucleating particles. *Proc. Natl. Acad. Sci. U.S.A.* **2016**, *113* (21), 5797-5803.

37. Burrows, S. M.; Hoose, C.; Poschl, U.; Lawrence, M. G. Ice nuclei in marine air: biogenic particles or dust? *Atmos. Chem. Phys.* **2013**, *13* (1), 245-267.

38. Vergara-Temprado, J.; Murray, B. J.; Wilson, T. W.; O'Sullivan, D.; Browse, J.; Pringle, K. J.; Ardon-Dryer, K.; Bertram, A. K.; Burrows, S. M.; Ceburnis, D.; DeMott, P. J.; Mason, R. H.; O'Dowd, C. D.; Rinaldi, M.; Carslaw, K. S. Contribution of feldspar and marine organic aerosols to global ice nucleating particle concentrations. *Atmos. Chem. Phys.* **2017**, *17* (5), 3637-3658.

39. Knulst, J. C.; Rosenberger, D.; Thompson, B.; Paatero, J. Intensive sea surface microlayer investigations of open leads in the pack ice during Arctic Ocean 2001 expedition. *Langmuir* **2003**, *19* (24), 10194-10199.

40. Schlitzer, R. *Ocean Data View*, <http://odv.awi.de>: 2014.

41. Dittmar, T.; Koch, B.; Hertkorn, N.; Kattner, G. A simple and efficient method for the solid-phase extraction of dissolved organic matter (SPE-DOM) from seawater. *Limnology and Oceanography-Methods* **2008**, *6*, 230-235.

42. Longnecker, K. Dissolved organic matter in newly formed sea ice and surface seawater. *Geochim. Cosmochim. Acta* **2015**, *171*, 39-49.

43. McIntyre, C.; McRae, C. Proposed guidelines for sample preparation and ESI-MS analysis of humic substances to avoid self-esterification. *Organic Geochemistry* **2005**, *36* (4), 543-553.

44. Bateman, A. P.; Walser, M. L.; Desyaterik, Y.; Laskin, J.; Laskin, A.; Nizkorodov, S. A. The effect of solvent on the analysis of secondary organic aerosol using electrospray ionization mass spectrometry. *Environ. Sci. Technol.* **2008**, *42* (19), 7341-7346.

45. Flerus, R.; Koch, B. P.; Schmitt-Kopplin, P.; Witt, M.; Kattner, G. Molecular level investigation of reactions between dissolved organic matter and extraction solvents using FT-ICR MS. *Mar. Chem.* **2011**, *124* (1-4), 100-107.

46. Stein, A. F.; Draxler, R. R.; Rolph, G. D.; Stunder, B. J. B.; Cohen, M. D.; Ngan, F. NOAA's HYSPLIT atmospheric transport and dispersion modeling system. *Bulletin American Meteorological Society* **2015**, *96*, 2059-2077.

47. Kujawinski, E. B.; Longnecker, K.; Blough, N. V.; Del Vecchio, R.; Finlay, L.; Kitner, J. B.; Giovannoni, S. J. Identification of possible source markers in marine dissolved organic matter using ultrahigh resolution mass spectrometry. *Geochim. Cosmochim. Acta* **2009**, *73* (15), 4384-4399.

48. Hertkorn, N.; Harir, M.; Koch, B. P.; Michalke, B.; Schmitt-Kopplin, P. High-field NMR spectroscopy and FTICR mass spectrometry: powerful discovery tools for the molecular level characterization of marine dissolved organic matter. *Biogeosciences* **2013**, *10* (3), 1583-1624.

49. Hawkes, J. A.; Hansen, C. T.; Goldhammer, T.; Bach, W.; Dittmar, T. Molecular alteration of marine dissolved organic matter under experimental hydrothermal conditions. *Geochim. Cosmochim. Acta* **2016**, *175*, 68-85.

50. Schmitt-Kopplin, P.; Liger-Belair, G.; Koch, B. P.; Flerus, R.; Kattner, G.; Harir, M.; Kanawati, B.; Lucio, M.; Tziotis, D.; Hertkorn, N.; Gebefugi, I. Dissolved organic matter in sea spray: a transfer study from marine surface water to aerosols. *Biogeosciences* **2012**, *9* (4), 1571-1582.

719 51. Stubbins, A.; Spencer, R. G. M.; Chen, H. M.; Hatcher, P. G.; Mopper, K.;
 720 Hernes, P. J.; Mwamba, V. L.; Mangangu, A. M.; Wabakanghanzi, J. N.; Six, J.
 721 Illuminated darkness: Molecular signatures of Congo River dissolved organic
 722 matter and its photochemical alteration as revealed by ultrahigh precision mass
 723 spectrometry. *Limnol. Oceanogr.* **2010**, *55* (4), 1467-1477.
 724 52. Gurganus, S. C.; Wozniak, A. S.; Hatcher, P. G. Molecular characteristics of
 725 the water soluble organic matter in size-fractionated aerosols collected over the
 726 North Atlantic Ocean. *Mar. Chem.* **2015**, *170*, 37-48.
 727 53. Kujawinski, E. B.; Behn, M. D. Automated analysis of electrospray
 728 ionization Fourier transform ion cyclotron resonance mass spectra of natural
 729 organic matter. *Anal. Chem.* **2006**, *78* (13), 4363-4373.
 730 54. Wozniak, A. S.; Bauer, J. E.; Sleighter, R. L.; Dickhut, R. M.; Hatcher, P. G.
 731 Technical Note: Molecular characterization of aerosol-derived water soluble
 732 organic carbon using ultrahigh resolution electrospray ionization Fourier
 733 transform ion cyclotron resonance mass spectrometry. *Atmos. Chem. Phys.* **2008**,
 734 *8* (17), 5099-5111.
 735 55. Andrews, S. J.; Hackenberg, S. C.; Carpenter, L. J. Technical Note: A fully
 736 automated purge and trap GC-MS system for quantification of volatile organic
 737 compound (VOC) fluxes between the ocean and atmosphere. *Ocean Sci.* **2015**, *11*
 738 (2), 313-321.
 739 56. Dittmar, T.; Whitehead, K.; Minor, E. C.; Koch, B. P. Tracing terrigenous
 740 dissolved organic matter and its photochemical decay in the ocean by using
 741 liquid chromatography/mass spectrometry. *Mar. Chem.* **2007**, *107* (3), 378-387.
 742 57. Flerus, R.; Lechtenfeld, O. J.; Koch, B. P.; McCallister, S. L.; Schmitt-Kopplin,
 743 P.; Benner, R.; Kaiser, K.; Kattner, G. A molecular perspective on the ageing of
 744 marine dissolved organic matter. *Biogeosciences* **2012**, *9* (6), 1935-1955.
 745 58. Gonsior, M.; Peake, B. M.; Cooper, W. T.; Podgorski, D. C.; D'Andrilli, J.;
 746 Dittmar, T.; Cooper, W. J. Characterization of dissolved organic matter across the
 747 Subtropical Convergence off the South Island, New Zealand. *Mar. Chem.* **2011**,
 748 *123* (1), 99-110.
 749 59. Kujawinski, E. B.; Longnecker, K.; Barott, K. L.; Weber, R. J. M.; Kido Soule,
 750 M. C. Microbial Community Structure Affects Marine Dissolved Organic Matter
 751 Composition. *Frontiers in Marine Science* **2016**, *3* (45).
 752 60. Knopf, D. A.; Alpert, P. A.; Wang, B.; Aller, J. Y. Stimulation of ice nucleation
 753 by marine diatoms. *Nat. Geosci.* **2011**, *4* (2), 88-90.
 754 61. Schnell, R. C. Ice nuclei produced by laboratory cultured marine
 755 phytoplankton. *Geophys. Res. Lett.* **1975**, *2* (11), 500-502.
 756 62. Fall, R.; Schnell, R. C. Association of an ice-nucleating pseudomonad with
 757 cultures of the marine dinoflagellate, *Heterocapsa niei*. *J. Mar. Res.* **1985**, *43* (1),
 758 257-265.
 759 63. Ladino, L. A.; Yakobi-Hancock, J. D.; Kalthau, W. P.; Mason, R. H.; Si, M.; Li,
 760 J.; Miller, L. A.; Schiller, C. L.; Huffman, J. A.; Aller, J. Y.; Knopf, D. A.; Bertram, A. K.;
 761 Abbatt, J. P. D. Addressing the ice nucleating abilities of marine aerosol: A
 762 combination of deposition mode laboratory and field measurements. *Atmos.*
 763 *Environ.* **2016**, *132*, 1-10.
 764 64. McCluskey, C. S.; Hill, T. C. J.; Malfatti, F.; Sultana, C. M.; Lee, C.; Santander,
 765 M. V.; Beall, C. M.; Moore, K. A.; Cornwell, G. C.; Collins, D. B.; Prather, K. A.;
 766 Jayarathne, T.; Stone, E. A.; Azam, F.; Kreidenweis, S. M.; DeMott, P. J. A Dynamic
 767 Link between Ice Nucleating Particles Released in Nascent Sea Spray Aerosol and

768 Oceanic Biological Activity during Two Mesocosm Experiments. *Journal of the*
769 *Atmospheric Sciences* **2017**, 74 (1), 151-166.

770 65. Wang, X. F.; Sultana, C. M.; Trueblood, J.; Hill, T. C. J.; Malfatti, F.; Lee, C.;
771 Laskina, O.; Moore, K. A.; Beall, C. M.; McCluskey, C. S.; Cornwell, G. C.; Zhou, Y. Y.;
772 Cox, J. L.; Pendergraft, M. A.; Santander, M. V.; Bertram, T. H.; Cappa, C. D.; Azam,
773 F.; DeMott, P. J.; Grassian, V. H.; Prather, K. A. Microbial Control of Sea Spray
774 Aerosol Composition: A Tale of Two Blooms. *Acs Central Science* **2015**, 1 (3),
775 124-131.

776 66. Compiano, A. M.; Romano, J. C.; Garabetian, F.; Laborde, P.; Delagiraudiere,
777 I. Monosaccharide composition of particulate hydrolyzable sugar fraction in
778 surface microlayers from brackish and marine waters. *Mar. Chem.* **1993**, 42 (3-
779 4), 237-251.

780 67. Aller, J. Y.; Kuznetsova, M. R.; Jahns, C. J.; Kemp, P. F. The sea surface
781 microlayer as a source of viral and bacterial enrichment in marine aerosols.
782 *Journal of Aerosol Science* **2005**, 36 (5-6), 801-812.

783 68. Miralto, A.; Barone, G.; Romano, G.; Poulet, S. A.; Ianora, A.; Russo, G. L.;
784 Buttino, I.; Mazzarella, G.; Laabir, M.; Cabrini, M.; Giacobbe, M. G. The insidious
785 effect of diatoms on copepod reproduction. *Nature* **1999**, 402 (6758), 173-176.

786 69. Stonik, V.; Stonik, I. Low-Molecular-Weight Metabolites from Diatoms:
787 Structures, Biological Roles and Biosynthesis. *Marine Drugs* **2015**, 13 (6), 3672.

788 70. Prestegard, S.; Erga, S.; Steinrücken, P.; Mjøs, S.; Knutsen, G.; Rohloff, J.
789 Specific Metabolites in a *Phaeodactylum tricornutum* Strain Isolated from
790 Western Norwegian Fjord Water. *Marine Drugs* **2016**, 14 (1), 9.

791 71. Wichard, T.; Pohnert, G. Formation of halogenated medium chain
792 hydrocarbons by a lipoxygenase/hydroperoxide halolyase-mediated
793 transformation in planktonic microalgae. *Journal of the American Chemical*
794 *Society* **2006**, 128 (22), 7114-7115.

795 72. Pohnert, G. Wound-activated chemical defense in unicellular planktonic
796 algae. *Angewandte Chemie-International Edition* **2000**, 39 (23), 4352-+.

797 73. Wolfe, G. V.; Steinke, M.; Kirst, G. O. Grazing-activated chemical defence in
798 a unicellular marine alga. *Nature* **1997**, 387 (6636), 894-897.

799 74. Cochran, R. E.; Laskina, O.; Jayarathne, T.; Laskin, A.; Laskin, J.; Lin, P.;
800 Sultana, C.; Lee, C.; Moore, K. A.; Cappa, C. D.; Bertram, T. H.; Prather, K. A.;
801 Grassian, V. H.; Stone, E. A. Analysis of Organic Anionic Surfactants in Fine and
802 Coarse Fractions of Freshly Emitted Sea Spray Aerosol. *Environ. Sci. Technol.*
803 **2016**, 50 (5), 2477-2486.

804 75. Bruggemann, M.; Hayeck, N.; Bonnineau, C.; Pesce, S.; Alpert, P. A.; Perrier,
805 S.; Zuth, C.; Hoffmann, T.; Chen, J.; George, C. Interfacial photochemistry of
806 biogenic surfactants: a major source of abiotic volatile organic compounds.
807 *Faraday Discussions* **2017**, 200, 59-74.

808 76. Zhou, S.; Gonzalez, L.; Leithead, A.; Finewax, Z.; Thalman, R.; Vlasenko, A.;
809 Vagle, S.; Miller, L. A.; Li, S. M.; Burekul, S.; Furutani, H.; Uematsu, M.; Volkamer,
810 R.; Abbatt, J. Formation of gas-phase carbonyls from heterogeneous oxidation of
811 polyunsaturated fatty acids at the air-water interface and of the sea surface
812 microlayer. *Atmos. Chem. Phys.* **2014**, 14 (3), 1371-1384.

813 77. Hung, H. M.; Ariya, P. Oxidation of oleic acid and oleic acid/sodium
814 chloride(aq) mixture droplets with ozone: Changes of hygroscopicity and role of
815 secondary reactions. *J. Phys. Chem. A* **2007**, 111 (4), 620-632.

816 78. Kind, T.; Fiehn, O. Metabolomic database annotations via query of
817 elemental compositions: Mass accuracy is insufficient even at less than 1 ppm.
818 *Bmc Bioinformatics* **2006**, 7, 10.
819 79. Tolić, N.; Liu, Y.; Liyu, A.; Shen, Y.; Tfaily, M. M.; Kujawinski, E. B.;
820 Longnecker, K.; Kuo, L.-J.; Robinson, E. W.; Paša-Tolić, L.; Hess, N. J. Formularity:
821 Software for Automated Formula Assignment of Natural and Other Organic
822 Matter from Ultrahigh-Resolution Mass Spectra. *Anal. Chem.* **2017**, 89 (23),
823 12659-12665.
824
825